THE JOURNAL OF BIOLOGICAL CHEMISTRY VOL. 281, NO. 14, pp. 9738–9744, April 7, 2006

Laboratory-evolved Vanadium Chloroperoxidase Exhibits 100-Fold Higher Halogenating Activity at Alkaline pH

*CATALYTIC EFFECTS FROM FIRST AND SECOND COORDINATION SPHERE MUTATIONS**

Received for publication, November 11, 2005, and in revised form, January 17, 2006 Published, JBC Papers in Press, February 2, 2006, DOI 10.1074/jbc.M512166200

Zulfiqar Hasan[‡], Rokus Renirie[‡], Richard Kerkman[§], Harald J. Ruijssenaars[‡], Aloysius F. Hartog[‡], and Ron Wever[‡1]

From the [‡]Van't Hoff Institute of Molecular Sciences, University of Amsterdam, 1018 WS Amsterdam, The Netherlands and [§]Dutch States Mines Anti-Infectives B.V., Delft, The Netherlands

Directed evolution was performed on vanadium chloroperoxidase from the fungus *Curvularia inaequalis* to increase its brominating activity at a mildly alkaline pH for industrial and synthetic applications and to further understand its mechanism. After successful expression of the enzyme in *Escherichia coli*, two rounds of screening and selection, saturation mutagenesis of a "hot spot," and rational recombination, a triple mutant (P395D/L241V/T343A) was obtained that showed a 100-fold increase in activity at pH 8 (k_{cat} = 100 s^{-1}). The increased K_m values for Br^- (3.1 mM) and H_2O_2 (16 μM) are smaller than those found for vanadium bromoperoxidases that are reasonably active at this pH. In addition the brominating activity at pH 5 was increased by a factor of 6 (k_{cat} = 575 s^{-1}), and the chlorinating activity at pH 5 was increased by a factor of 2 (k_{cat} = 36 s^{-1}), yielding the "best" vanadium haloperoxidase known thus far. The mutations are in the first and second coordination sphere of the vanadate cofactor, and the catalytic effects suggest that fine tuning of residues Lys-353 and Phe-397, along with addition of negative charge or removal of positive charge near one of the vanadate oxygens, is very important. Lys-353 and Phe-397 were previously assigned to be essential in peroxide activation and halide binding. Analysis of the catalytic parameters of the mutant vanadium bromoperoxidase from the seaweed *Ascophyllum nodosum* also adds fuel to the discussion regarding factors governing the halide specificity of vanadium haloperoxidases. This study presents the first example of directed evolution of a vanadium enzyme.

Haloperoxidases catalyze the oxidation of halides to hypohalous acids (see Equation 1), an industrially interesting reaction; these enzymes can be used to halogenate various organic compounds (1, 2) (see Equation 2). In addition they may provide an alternative biocide in antifouling applications (3–5) or may be used as a component in disinfectants and in detergent formulations for bleaching purposes (6–8). Equations 1 and 2 illustrate the reactions occuring.

$$H_2O_2 + X^- + H^+ \rightarrow HOX + H_2O \quad \text{(Eq. 1)}$$

$$HOX + AH \rightarrow AX + H_2O \quad \text{(Eq. 2)}$$

where X is clorine, bromine, or iodine, and A is an organic nucleophilic acceptor.

Presently two classes of enzymes are known that efficiently catalyze the oxidation of a halide by hydrogen peroxide, the vanadium haloperoxidases and the heme peroxidases. The heme peroxidases have a significant disadvantage of rapid inactivation during turnover because of an oxidative reaction of the heme group with the peroxide substrate and the formed hypohalous acids. Vanadium haloperoxidases (VHPOs),[2] which contain vanadate (VO_4^{3-}) as a prosthetic group, do not suffer from this disadvantage (9); in addition they are much more resistant toward heat, detergent, and solvent denaturation (10). The major drawback of all haloperoxidases including the stable VHPOs is that they are mainly active at mildly acidic pH values, whereas for many applications activity at mildly alkaline pH values is required. An example of this is their potential use as an antifouling agent in marine paints (3–5), an application inspired by their putative role *in vivo*. Many brown seaweeds contain vanadium haloperoxidases that are present on the plant surface (11), and apart from the direct antimicrobial activity of HOBr and HOCl it was demonstrated that these hypohalous acids react rapidly with homoserine lactone derivatives produced by bacteria as communication signals (quorum sensing) thus preventing biofilm formation on the surface of these seaweeds (12). Current antifouling technologies are often very environmentally unfriendly, but still being used because of the absence of good alternatives.

Crystal structures of VHPOs have shown peculiar vanadium chemistry: the enzymes shuttle between a trigonal bipyramidal structure (native) and a distorted tetragonal structure (peroxo-intermediate) (see Fig. 1). Despite considerable additional data (kinetic, genetic, mutational, and spectroscopic) on VHPOs from different organisms (16–18), several questions about these enzymes remain to be answered. Especially the factors governing the halide specificity and pH optima are not fully understood. Fig. 2 shows a picture emerging from three previously published proposals (14, 15, 19) on the differences between vanadium chloroperoxidases (VCPOs) and vanadium bromoperoxidases (VBPOs). It was suggested that binding of the halide in VCPO is assisted by residues Phe-397 and Trp-350 via their δ+ ring edge (19). The VBPOs have a histidine in the position corresponding to Phe-397 and the VBPOs from the marine algae *Corallina officinalis* and *Corallina pilulifera* have an arginine in the position of Trp-350 (17), thereby suggesting that differences in specificity may be partially explained by amino acid variations at these two positions. In addition to differences in direct binding of the halide, it was suggested that in the VBPO from the seaweed *Ascophyllum nodosum* the bound peroxide is deprotonated by His-411 (Fig. 2), thereby reducing the oxidative strength of these enzymes and their affinity for the halide (14). The assigned full positive charge on the protonated peroxide oxygen in VCPO was also suggested

* This work was supported by the Netherlands Organization for Scientific Research (NWO), The Netherlands Technology Foundation (STW), the Dutch National Research School Combination (NRSC-Catalysis), and DSM Research. The costs of publication of this article were defrayed in part by the payment of page charges. This article must therefore be hereby marked "*advertisement*" in accordance with 18 U.S.C. Section 1734 solely to indicate this fact.

[1] To whom correspondence should be addressed: Van't Hoff Institute of Molecular Sciences, University of Amsterdam, Nieuwe Achtergracht 129, 1018 WS Amsterdam, The Netherlands. Tel.: 31-20-5255110; Fax: 31-20-5255670; E-mail: rwever@science.uva.nl.

[2] The abbreviations used are: VHPO, vanadium haloperoxidase; VCPO, vanadium chloroperoxidase; VBPO, vanadium bromoperoxidase; epPCR, error-prone PCR; LB, Luria Broth medium; MCD, monochlorodimedone; FPLC, fast liquid protein chromatography.

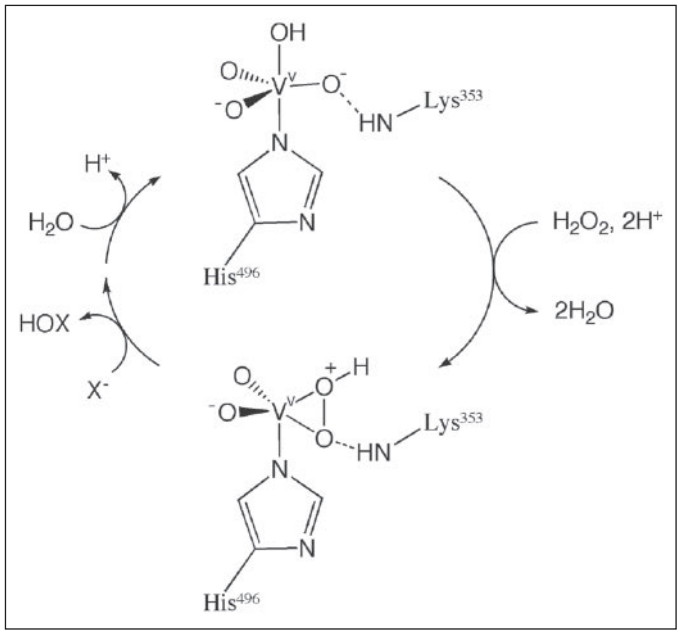

FIGURE 1. **Minimal scheme of the catalytic cycle of vanadium chloroperoxidase from the fungus *C. inaequalis* based on crystal structures of the native enzyme and the peroxo-intermediate (13).** The activated peroxo atom that reacts with the halide is proposed to be positively charged (14, 15).

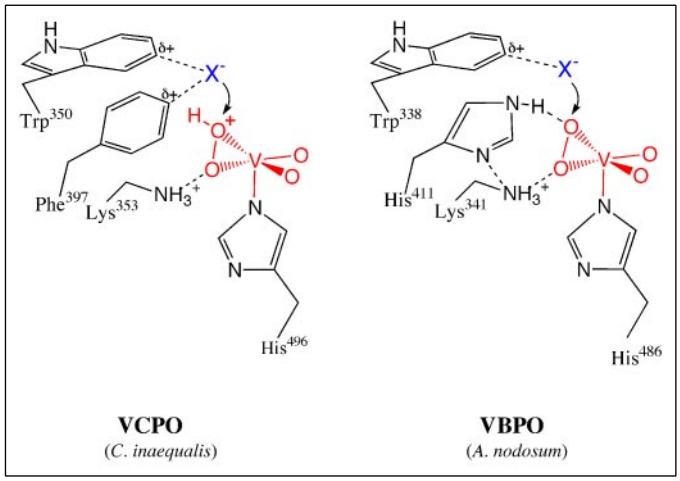

FIGURE 2. **Tuning of the activity of vanadium haloperoxidases from different origins.** Halide binding in VCPO was suggested to be assisted by residues Phe-397 and Trp-350 via their δ+ ring edge (19); VBPOs have a histidine in the position corresponding to Phe-397, and the VBPOs from *C. officinalis* and *C. pilulifera* have an arginine in the position of Trp-350 (17). In VBPO from *A. nodosum* the bound peroxide may be deprotonated by His-411, thereby reducing the oxidative strength of these enzymes and their affinity for the halide (14). The His-411 of VBPO from *A. nodosum* also forms a hydrogen bond with the catalytically important Lys-341 (15).

to give rise to the very strong uncompetitive inhibition by azide seen in VCPO, being absent in wild-type VBPOs (20). A VBPO mutant from *C. pilulifera* that essentially has become a VCPO was also strongly inhibited by azide (21). The His-411 of VBPO from *A. nodosum* also forms a hydrogen bond with the catalytically important Lys-341, and it was suggested that this decreases the polarizing effect of this histidine on the bound peroxide (15). A clear explanation for the pH profiles in these enzymes is lacking, but interestingly, the optima of the VBPOs are shifted to more neutral pH values (5.5–6.0) as compared with the VCPOs (pH 4.5–5.0). Attempts to rationally modify the properties of these enzymes by site-directed mutagenesis have only met limited success. Two variants of VCPO from the fungus *Curvularia inaequalis* with a reduced positive charge near the vanadate cofactor (R360A and R490A) showed higher brominating activity at alkaline pH; however these mutants inactivated during turnover and lost most of their ability to oxidize chloride (22). The most successful attempt to date has been a site-directed mutagenesis study in which substantial chlorinating activity (40 s^{-1}) was introduced in a VBPO from the marine algae *C. pilulifera* (mutants R397W and R397F); however the reported K_m values for Cl^- of two mutants were very high (~700 mM) (22).

In this study we have used directed evolution techniques to improve the activity of VCPO from *C. inaequalis* at mildly alkaline pH. This enzyme is evolutionarily related to the mentioned seaweed peroxidases, and a recombinant system for producing VCPO is available. Kinetic studies have shown that although the enzyme effectively oxidizes bromide (k_{cat} = 100 s^{-1}) at pH 5 it has a k_{cat} of only 1 s^{-1} at the slightly alkaline pH of seawater (pH 8) (22). In this study we obtained a VCPO triple mutant exhibiting 100-fold higher activity at pH 8, as well as an increase in the brominating and chlorinating activity at pH 5 by factors of 6 and 2, respectively. Apart from potential applications of this mutant, the results generate more fuel to the discussion about the role of various catalytic residues in these enzymes.

EXPERIMENTAL PROCEDURES

Expression of VCPO in Escherichia coli—We expressed VCPO in a TOP10 *E. coli* host expression system (Invitrogen) for efficient expression and screening of mutants. The cDNA encoding the VCPO gene was amplified from the *Saccharomyces cerevisiae* expression plasmid pTNT14 (22) using the forward primer 5′-CTGAGCTAGCCATATGGGGGTCCGTTACACCCATCC-3′ (NheI site underlined) and the reverse primer 5′-AAGGTACCCTACGGCGCCTCCTTGACTACCGG-3′ (KpnI site underlined) using *Pfu* turbo polymerase (Invitrogen). Following digestion with NheI and KpnI restriction enzymes the DNA was ligated into pBADgIIIB (Invitrogen) restricted with the same enzymes. This construct includes the gIII signal sequence to facilitate VCPO secretion into the *E. coli* periplasm. *E. coli* TOP10 cells were transformed with the construct pBADVCPO and plated onto LB agar (100 $\mu g \cdot ml^{-1}$ ampicillin). Single colonies were tested for expression by checking the phenol red bromination activity at pH 5.0. Optimum expression of VCPO was obtained by growing cells at 37 °C to an $A_{600\ nm}$ of 0.6–0.8, cooling cells to 25 °C and inducing with 0.02% L-arabinose, and growing for another 20–24 h. The expression of VCPO in *E. coli* yielded an enzyme production of 10 $mg \cdot liter^{-1}$ culture. The recombinant *E. coli* VCPO showed similar kinetic parameters to the previously recombinant enzyme that was expressed in the yeast *S. cerevisiae* (22), including the pH dependence of the bromide oxidation (pH 4–9 (not shown)).

Random Mutagenesis, Saturation Mutagenesis, and Site-directed Mutagenesis—The protein sequence space was explored by using the error-prone (ep)PCR (25, 26) as the mutagenesis method, using either the GeneMorph™ I or II kit (Stratagene). epPCR was performed on 1.3 Kb, thereby leaving out the 0.5 Kb 5′-end that codes for the N-terminal of the enzyme. This region is far removed from the catalytic core and is thought to be involved in the stability of VCPO. The primers used were the forward primer 5′-CCTCAACGATCCTCGAGGTGCTTCGC-3′ (XhoI site underlined) and the reverse primer 5′-CCATATGGTACCCTACGGCGCCTCCTTGACTACCGG-3′ (KpnI site underlined). An average frequency of 1.6 base changes per kilobase was verified by DNA sequencing (MWG Biotech AG) of 10 independent colonies. The amplified DNA was subcloned into the XhoI-KpnI digested pBAD-VCPO and transformed back into *E. coli* TOP10 cells. From an estimated library size of 2×10^4, 5000 colonies were robotically picked and

transferred to the 96-well format and grown in LB to prepare cells for glycerol stocks. For the second generation library, a similar procedure for library construction and preparation was followed, and 8000 colonies were screened. Saturation mutagenesis at Pro-395 residue was performed using the QuikChange™ kit (Stratagene). The oligonucleotide designs were based on the following set of primers, sense primer 5′-CAACGACATTCCATTCAAGNNNCCTTTCCCAGCTTACCC-3′ and antisense primer 5′-GGGTAAGCTGGGAAAGGNNNCTT-GAATGGAATGTCGTTGG-3′ using the optimal codon requirement (at positions underlined) for *E. coli* expression. The QuikChange™ kit was also used to construct the site-directed control mutants using the oligonucleotides, L241V (sense) 5′-CGCAGAGCGAGCACTTC*GTG*-GCCGACCCACCGGGCC-3′, L241V(antisense) 5′-GGCCCGGTGG-GTCGGC*CAC*GAAGTGCTCGCTCTGCG-3′; T343A (sense) 5′-CGTCGACGTCGCTTGC*GCA*GACGCTGGTATCTTTTCC-3′, T343A(antisense) 5′-GGAAAAGATACCAGCGTC*TGC*GCAAGC-GACGTCGACG-3′; R360C (sense) 5′-GGGAGTTCGAATTCTGG*T*-*GC*CCACTATCTGGTGTGCG-3′, R360C(antisense) 5′-CGCACAC-CAGATAGTGG*GCA*CCAGAATTCGAACTCCC-3′; A399S (sense) 5′-CCATTCAAGCCTCCTTTCCCA*TCT*TACCCATCTGGTCAC-GCGACC-3′, A399S(antisense) 5′-GGTCGCGTGACCAGATGGG-TA*AGA*TGGGAAAGGAGGCTTGAATGG-3′ (codons for amino acid are underlined, and mutagenesis position are in italics).

High Throughput Expression of VCPO Mutants—Cell growth and enzyme expression was performed in 2-ml volume, 96-well format polypropylene deep well plates (Greiner Bio-One). Using a 96-pin colony replicator, frozen cells were transferred to the deep well plates containing 1 ml of liquid LB medium with 100 $\mu g \cdot ml^{-1}$ ampicillin and 0.02% L-arabinose and covered with Breath Seal porous films (Greiner Bio-One). The cells were grown using an INFORS Microtron plate shaker for 24 h at 25 °C at 560 rpm. The plates were chilled to 4 °C and centrifuged at 3500 rpm (Beckmann S5700). The media were removed, the cells were washed with 50 mM Tris-SO_4, pH 8.3, lysed by resuspending and incubating in 100 μl of lysis buffer (50 $\mu g \cdot ml^{-1}$ Lysozyme, 40 Kunitz units$\cdot ml^{-1}$ DNase, 4 mM $MgSO_4$, 0.05% Triton X-100, 100 mM Tris-SO_4, pH 8.0) for 10 min, followed by a freeze-thaw cycle. The suspensions were then transferred to V-bottom microtiter plates and centrifuged as before. The supernatants were removed to fresh flat bottom microtiter plates, and aliquots were used for screening assays.

High Throughput Assay and Kinetic Analysis of the Most Promising Mutants—For the initial high throughput screening of mutants a phenol red-based assay was used (10). This assay exhibits a color change from deep pink to purple (bromphenol blue) upon bromination at pH 8.0. The assay conditions used for the initial screen were 1 mM Br^- (the concentration in seawater (27)), 10 mM H_2O_2, 100 μM vanadate (the enzyme is expressed as an apo-protein), 50 μM phenol red, and 100 mM Tris SO_4, pH 8.0. The hydrogen peroxide concentration in the initial screen was 10 times higher than that used in a standard VCPO assay to compensate for potential depletion of H_2O_2 by endogenous catalase in the cell lysates (28, 29). Enzyme dilutions and assays were performed by a Roboseq SE automated liquid handling system (MWG Biotech AG) and rates of phenol red bromination followed by a 96-well plate reader at 590 nm (Fluostar Galaxy, BMG Labtech). Aliquots of enzyme lysates (10 μl) were transferred to flat bottom microtiter plates, and a 90-μl phenol red solution (100 mM Tris SO_4, pH 8.0, 100 μM vanadate (sodium salt), 10 mM H_2O_2, 1 mM KBr, 50 μM phenol red) was added, and plates were vortexed at 500 rpm for 10 s. VCPO variants exhibiting increased phenol red bromination in the initial screen were sequenced and also reassayed using 50 μM monochlorodimedone (MCD) (2-chloro-5,5-dimethyl-1,3-dimedon), a more effective bromide acceptor (30, 31), to calculate precise turnover numbers. This reaction is followed spectrophotometrically by following the absorbance decrease at 290 nm ($\Delta\epsilon = 20\ mM^{-1}cm^{-1}$). From these mutants the four most active mutants were grown on a large scale and purified and reassayed with the MCD assay. Enzyme samples were transferred to quartz cuvettes (100 mM Tris SO_4, pH 8.0, 100 μM vanadate (sodium salt), 1 mM H_2O_2, 1 mM Br^-, 50 μM MCD). The halogenation rates were followed using a Cary 50 spectrophotometer.

Purification of Enzymes and Mutants—*S. cerevisiae* VCPO was produced and purified as described before (22). Purification of *E. coli* VCPO was similar to the *S. cerevisiae* VCPO; disruption of the yeast cells by glass beads was replaced by sonication of the *E. coli* cells. In addition, the last FPLC step from the *S. cerevisiae* VCPO purification was omitted because it did not result in further purification of the *E. coli* VCPO. VBPO from the seaweed *A. nodosum* was harvested and purified as described before (32).

RESULTS

E. coli Expression System and Generation of Mutants—For our directed evolution, expression of VCPO in an *E. coli* host was desirable. Our VCPO was successfully expressed, yielding an enzyme production of 10 $mg \cdot liter^{-1}$ culture, sufficient for convenient high throughput screening. In the past expression of vanadium haloperoxidases in *E. coli* was cumbersome and only low levels of protein expression were obtained due to inclusion body formation (0.1–0.3 mg/liter culture for VBPO from *C. officinalis* (23)) and a very low yield for VBPO from *C. pilulifera* (24). We optimized our system by inducing the cells at 25 °C, similar to the study of recombinant VBPO from *C. officinalis* (23); however our yield of soluble active protein was much higher. For the *Corallina* VBPOs the more difficult expression is probably because of the fact that they are dodecameric enzymes as opposed to the monomeric VCPO. For the dimeric VBPO from *A. nodosum* expression is also difficult because of the presence of inter- and intramolecular disulfide bonds.

Error-prone PCR mutagenesis was then successfully used to create VCPO mutant libraries and DNA sequence analysis revealed 1.1 amino acid changes on average per mutant. Screening of 5×10^3 mutants in round one and 8×10^3 in round two was performed using a phenol red-based assay (1 mM Br^-, pH 8.0) to identify variant enzymes with enhanced bromination activity. Table 1 summarizes the results of two rounds of screening, saturation mutagenesis of hot spot residue Pro-395, and rational recombination of selected mutants.

Analysis of Mutants—Ultimately the best mutant generated was the triple mutant P395D/L241V/T343A with a 40-times-increased brominating activity under our screening conditions (1 mM Br^-). Fig. 3 depicts the peroxo-intermediate of the enzyme showing that the mutated residues are in close proximity to the VCPO active site residues. Pro-395 showed up as a hot spot in the first generation; a P395T mutant and a P395H/A399S double mutant were found (Table 1). Fig. 4 shows that Pro-395 borders the active site channel and neighbors Phe-397, a residue that is believed to be a part of the halide-binding site (19). Mutation of Pro-395 may influence both the electrostatics in the vicinity of Phe-397 (influencing its $\delta-/\delta+$ distribution) and the orientation of Phe-397, either directly or via increased backbone flexibility. Ala-399 is also close to Phe-397; however a A399S control mutant only showed a small increase in activity compared with wild type. In addition, a generated P395H mutant had a similar activity as the P395H/A399S mutant, excluding an important role for the A399S mutation.

The other mutant from the first generation, R360C/I391V, indicated a second hot spot. An R360A mutant previously generated by site-di-

rected mutagenesis also exhibited a higher activity at alkaline conditions (22). An R360C control mutant was identical to the R360C/I391V variant (not shown), excluding an important role for the I391V mutation. Arg-360 has an important role in binding the vanadate cofactor, and, interestingly, also stabilizes the position of Phe-397 by forming a hydrogen bond to its carbonyl group, as shown in Fig. 5. In fact, the crystal structure of R360A mutant shows that the torsion angle of the Phe-397 ring changes as a result of the mutation (34). Thus both mutated residues from the first round of screening (Pro-395 and Arg-360) may influence the position or orientation of Phe-397. This residue was previously suggested to support halide binding via its δ+ ring edge (Fig. 2, *left panel*), as also observed in haloalkane dehalogenases (35). In this respect it is interesting to note that in our final mutant a higher bromide concentration is required than in the wild type to reach a maximal activity (Table 2).

TABLE 1
VCPO mutants with enhanced activity at alkaline pH obtained by directed evolution

Mutant	Activity enhancement factor at pH 8.0[a]
Wild-type VCPO	1
First generation[b]	
R360C/I391V	5
P395H/A399S	5
P395T	6
Second generation[c]	
P395T/T343A	14
P395T/L241V	19
Saturation mutagenesis[b]	
P395D	10
P395E	10
Recombined mutants[c]	
P395T/L241V/T343A	20
P395D/L241V/T343A (1 mM Br^-)	40
P395D/L241V/T343A (100 mM Br^-)	100
Control mutants[b]	
R360C	5
A399S	1.2
T343A	4
L241V	7

[a] Assay conditions 1 mM H_2O_2, 1 mM Br^-, 100 μM vanadate, 50 μM MCD, 100 mM $TrisSO_4$, pH 8.0.
[b] Cell lysates.
[c] Purified enzyme.

Unfortunately, the R360C/I391V mutant inactivates during turnover (as was also previously observed for the R360A mutant (22)), possibly because of loss of cofactor during turnover, eliminating application of this mutation. Therefore a Pro-395 mutant (P395T) was chosen as the starting point for a second round of epPCR. Simultaneously, the Pro-395 position was investigated by saturation mutagenesis of this residue. From the 19 Pro-395 saturation mutants constructed, P395D and P395E were most active, both exhibiting a 10-fold higher activity than wild type. This result suggests that introducing a negative charge at this position leads to a higher activity at pH 8, possibly by influencing pK_a values and/or the position of essential catalytic groups. The second round of epPCR (Table 1) generated two mutants with further increases in activity, P395T/L241V (19-fold) and P395T/T343A (14-fold). A site-directed mutant carrying only the L241V mutation showed a 7-fold enhancement as compared with the wild-type enzyme, whereas a T343A single mutant showed a 4-fold increase, indicating that these mutations are synergistic with the P395T mutation. In the x-ray structure of the native enzyme (13) Leu-241 is found in van der Waals contact with Glu-352, a residue next to the catalytically crucial Lys-353 (Fig. 3). This lysine forms a strong hydrogen bond (2.67 Å) to one of the peroxo-oxygen atoms of the peroxo-intermediate, and it is generally believed that this hydrogen bond induces bond polarization necessary for heterolytic cleavage of the side-on-bound peroxide. Previous site-directed mutagenesis studies have confirmed that this residue is crucial for activity (22). Fig. 3 shows that Thr-343 is reasonably close to the vanadate cofactor; however the rationale behind the effect of the T343A mutation is not clear.

After the second round and the saturation mutagenesis, a combinatorial study was carried out in which the interesting mutations were recombined. The purified mutants P395T/L241V/T343A and P395D/L241V/T343A showed a 20- and 40-fold enhancement, respectively.

Kinetic Characterization of the Mutant P395D/L241V/T343A—We performed a more detailed kinetic study of the best mutant (P395D/L241V/T343A) (Table 2) and compared it with VBPO from *A. nodosum* that naturally evolved at pH 8 and 1 mM Br^-. Our results show that by increasing the Br^- concentration the brominating activity can be further increased. At 100 mM Br^- the activity is 2.5-fold higher than the same mutant at 1 mM Br^- and thus 100-fold higher than wild-type VCPO. This further increase in activity going from 1 to 100 mM Br^- is caused by the fact that 1 mM Br^- does not represent V_{max} conditions for

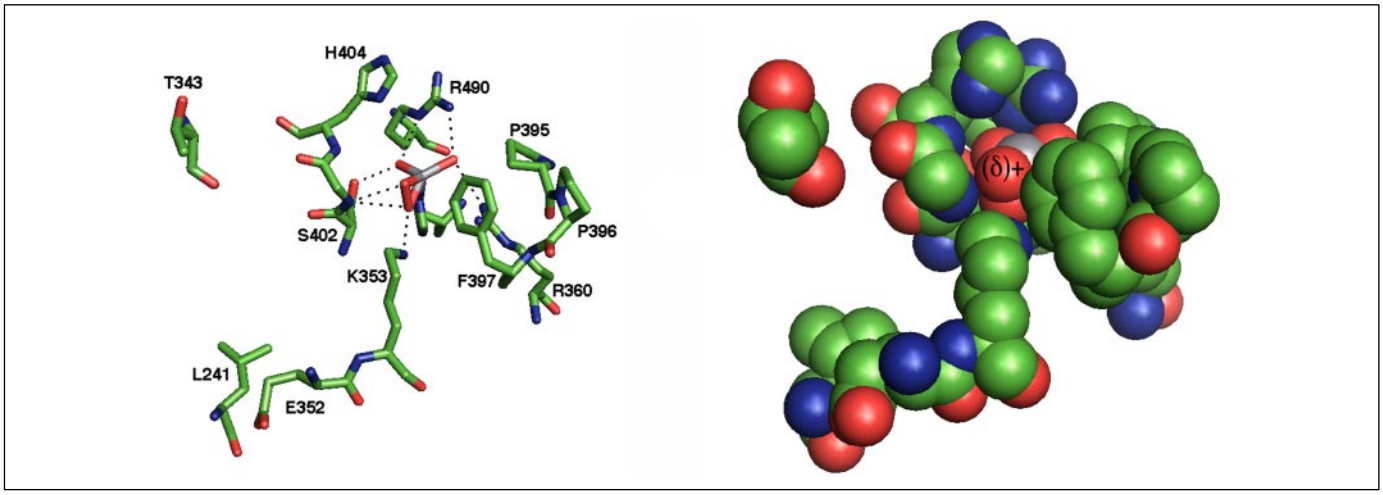

FIGURE 3. **Crystal structure of the catalytic peroxo-intermediate of vanadium chloroperoxidase (PDB code 1IDU), showing the cofactor environment including the residues altered in the directed evolution mutant P395D/L241V/T343A.** The vanadium atom is shown in *gray*. The panel on the right shows a space-filling representation: the activated peroxide oxygen (14) that reacts with the halide is labeled (δ)+ (see also Fig. 1). This figure was made with PyMOL (33).

the P395D/L241V/T343A mutant (K_m = 3.1 mM, Table 2), whereas for the wild-type it does (K_m = 0.12 mM, Table 2). This K_m value for Br^- is still smaller than that of VBPO from *A. nodosum* (16 mM). The large gain in activity has partially occurred at the expense of the very low K_m value, so the effect in terms of V_{max}/K_m is modest (factor 4). Our assay in the high throughput screening was carried out in the presence of 100 μM vanadate, and therefore formation of a mutant with a decreased affinity for vanadate may have gone unnoticed. However, reactivation studies of the apo-mutant in seawater (concentration vanadate in seawater ~50 nM) (37) showed that it rapidly and completely reactivated (not shown). Our initial high throughput screening at 10 mM H_2O_2 also harbors the potential danger that the high affinity of the wild-type enzyme for this substrate (<5 μM) is lost upon mutation. Although a K_m value of 16 μM for the P395D/L241V/T343A mutant represents a slight increase, it is still small and of similar magnitude as for VBPO from *A. nodosum* (22 μM). All together, at 1 mM Br^- the P395D/L241V/T343A mutant is maximally 40 times more active then wild-type VCPO and 8 times more active than VBPO from *A. nodosum*.

In addition to the results obtained at pH 8, the P395D/L241V/T343A mutant was investigated at pH 5 (Table 2). The brominating activity of this mutant at pH 5 is increased ~6-fold to a k_{cat} of 575 s^{-1}, which is one of the highest values for Br^- turnover reported for a vanadium haloperoxidase. The chlorinating activity of the P395D/L241V/T343A mutant is ~2-fold higher than the wild-type enzyme, thereby making this the best chlorinating vanadium haloperoxidase (21, 22).

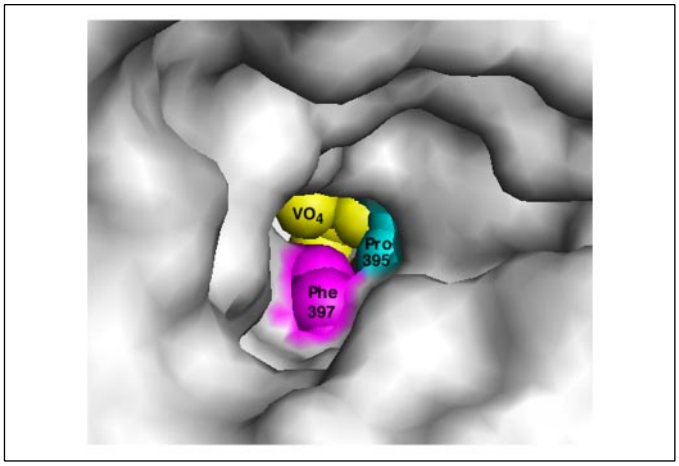

FIGURE 4. **View of the active site channel of VCPO showing the position of Pro-395, mutation of which to several residues (aspartic acid and glutamic acid in particular) leads to increased activity at pH 8.** The vanadate cofactor (*VO_4*), Pro-395, and Phe-397 are shown as *spheres*, whereas the surrounding residues are shown as surface. In addition to electrostatic effects on the vanadate oxygens and the putative halide-binding residue Phe-397, increased flexibility of Phe-397 may explain the observed tuning of the activity. This figure was made with PyMOL (33).

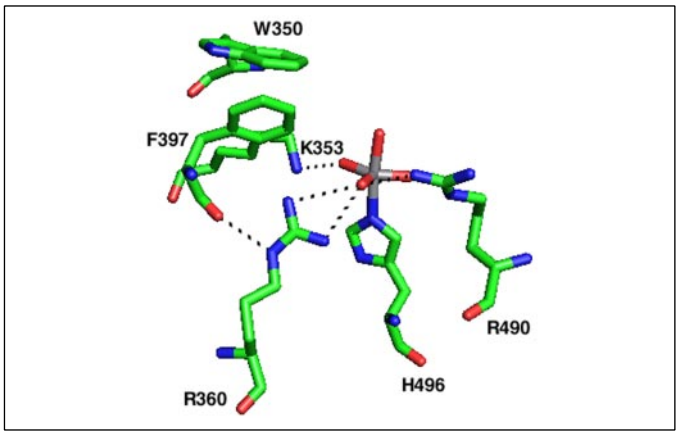

FIGURE 5. **The active site of native VCPO showing the proximity of Arg-360 with Phe-397.**

DISCUSSION

Two important issues on vanadium haloperoxidases that remain unsolved are their halide specificity and the factors that govern their pH profiles. Some insight into the halide specificity has been obtained from site-directed mutagenesis studies (22) and by comparison of crystal structures (17, 19) identifying Phe-397 and Trp-350 and the corresponding residues in VBPOs as putative halide-binding residues. In VBPOs a histidine residue is found on the position of Phe-397, whereas in *Corallina* VBPOs an arginine is found in the position of Trp-350. However, a clear hypothesis on the origin and differences of the pH profiles of these enzymes is lacking. Because there is an intricate interplay of hydrogen bonds and charges in the active site, rational changes of the pH profile and halide-binding characteristics by site-directed mutagenesis are difficult to predict. Therefore, we used directed evolution as the approach to obtain variants with enhanced activity at high pH. We chose screening conditions of 1 mM Br^- and pH 8, to ensure retention of sufficient affinity for bromide and to resemble seawater conditions. As outlined under "Results" the two hot spots from the first generation of directed evolution mutants, Pro-395 and Arg-360, both point toward tuning of Phe-397. Both the Pro-395 and Arg-360 mutants as well as our final mutant require a higher bromide concentration than the wild-type VCPO to reach a maximal activity, in line with the halide-binding site being affected. These results are also in line with studies on VBPO from *A. nodosum* (Table 2) that has a histidine (His-411) in the position corresponding to Phe-397 as illustrated in Fig. 2. Like our mutants, VBPO needs a higher bromide concentration than VCPO to reach maximal turnover. In addition it was previously shown that a F397H mutation in VCPO affected the affinity for the halide, as the K_m values for Cl^- and Br^- were increased ~10-fold (38). All these obser-

TABLE 2

Detailed kinetic analysis of VCPO mutant P395D/L241V/T343A obtained by directed evolution and comparison with wild-type VCPO and VBPO from *A. nodosum* (100 μM vanadate, 50 μM MCD)

N.D., not determined. Also, the chlorinating activity at pH 8 was not assayed, because the K_m for Cl^- at high pH for these VHPOs is impractically high (up to 1 M).

Enzyme	Oxidation Br^- (1 mM Br^-) pH 8.0	Oxidation Br^- (100 mM Br^-) pH 8.0	K_m (Br^-) (1 mM H_2O_2) pH 8.0	K_m (H_2O_2) (1 mM Br^-) pH 8.0	Oxidation Br^- (0.5 mM Br^-)[a] pH 5.0	Oxidation Cl^- (5 mM Cl^-)[a] pH 5.0
	s^{-1}	s^{-1}			s^{-1}	s^{-1}
Wild-type VCPO	1	1	0.12 mM	<5 μM[b]	100	20
P395D/L241V/T343 A mutant	40	100	3.1 mM	16 μM	575	36
VBPO (*A. nodosum*)	5	50	16 mM[c]	22 μM[d]	N.D.	≪1

[a] 1 mm H_2O_2.
[b] Because of the sensitivity limit of the MCD assay only an upper limit of 5 μM can be given.
[c] Taken from literature (36), the other VBPO values in this table were reassayed and found similar to previously published values (36).
[d] For VBPO from *C. pilulifera* the K_m value for Br^- is 8.4 mM at pH 6.5 (21).

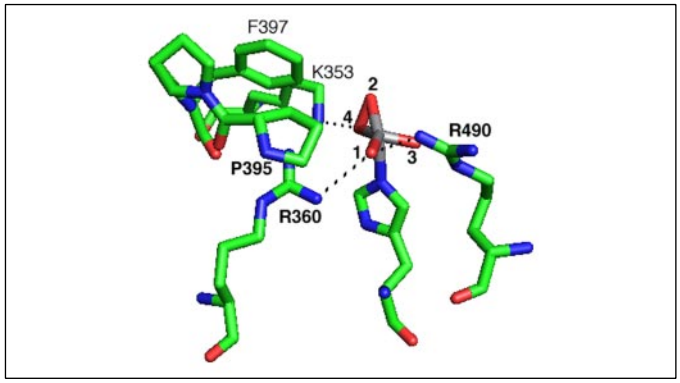

FIGURE 6. **Position of residues Pro-395, Arg-360, and Arg-490 in relation to the vanadate cofactor.** The vanadate oxygens are numbered *1–4*, according to Ref. 13. Mutation of these residues leads to electrostatic changes near the vanadate cofactor, partially explaining the increased activity of VCPO mutants at high pH. Either the introduction of negative charge at Pro-395 (P395D and P395E variants) or the removal of positive charge (R360C, R360A, and R490A mutants (22, 34)) may influence the charge on vanadate oxygen-1 and thereby the entire cofactor. Mutation of either Arg-360 or Arg-490 is too drastic because activity is lost during turnover. This figure was made with PyMOL (33).

vations support the hypothesis that tuning Phe-397 is crucial for the activity of VCPO. In addition to the identity and the position of this residue, the charge effects on Phe-397 may be crucial; mutagenesis of Pro-395 that is next to Phe-397 (Fig. 4) has the largest effect if a negative charge is introduced. Introducing a negative charge at the Pro-395 position may also have repelling effect on the halide, in agreement with the observed demand for a higher halide concentration. It is interesting to note that Lys-353 is located close to Phe-397; recently it was suggested that the polarization effect of the corresponding lysine in VBPO is tuned by a hydrogen bond to His-411 (15), the residue that corresponds to Phe-397 in VCPO (Fig. 2). Because VBPO is more active at high pH than VCPO this is in line with our explanation that mutations influencing the position of Lys-353 in VCPO are responsible for changes in enzymatic activity.

In addition to tuning the position and electrostatics in the vicinity of Phe-397 the altered activity observed in the Pro-395 and Arg-360 mutants can be explained by a change in the electron density on the vanadate oxygens. Fig. 6 shows that both Pro-395 and Arg-360 are in close contact with vanadate oxygen-1. Introducing a negative charge at Pro-395 or the removal of the positive charge of Arg-360 will influence the charge on the vanadate oxygens including oxygen-2 that is believed to be transferred to the halide during catalysis. This idea is supported by a previous observation (22) describing an R490A mutant of VCPO that also exhibited a similar increased activity at high pH; Fig. 6 shows that also Arg-490 is in close contact with vanadate oxygen-1. Influencing vanadate oxygen-1 will affect the entire cofactor, which then may lead to pK_a changes of crucial groups in catalysis, *e.g.* that of vanadate oxygen-2. This may partially account for the observed higher activity at pH 8. The increased electron density on vanadate oxygen may also attribute to the observed demand for a higher halide concentration to reach maximal turnover rates. Similar arguments can be used for the tuning effect of Lys-353 as described under "Results." All of the effects described above may strengthen each other concertedly. Previously, x-ray structures of five active site mutant VCPOs and the apo-form of the enzyme were determined, showing no changes in the secondary structure. These investigations have shown that the secondary structure of VCPO is very rigid, strongly decreasing the likelihood of large changes in the P395D/L241V/T343A mutant. Our error-prone PCR strategy was designed for maximal retention of protein stability, as we did not subject the structurally important N-terminal residues to mutagenesis. Moreover, we have shown that the cofactor vanadate is still strongly bound in this mutant, also suggesting correct folding. X-ray structure determination of the mutant will have to identify subtle changes and show whether our interpretations of the kinetic results are correct.

At 1 mM Br^- and pH 8 the P395D/L241V/T343A mutant shows a much higher activity than both the wild-type VCPO and VBPO from *A. nodosum*, making this mutant a good candidate for antifouling applications in seawater. In disinfection and synthetic applications higher concentrations of Br^- may be used, thereby employing the maximal turnover of the mutant. As an example of the latter, we intend to couple alkaline halogenation of aromatic compounds by the mutant to a palladium-catalyzed Heck reaction (39, 40), which only occurs effectively at alkaline pH. In this manner the halide is recycled thus leading to elimination of salt waste.

Our work may raise the question of why these simple variants were not made by the natural organisms themselves, because it is believed that the formation of hypohalous acids is the natural role of these enzymes. The most obvious answer to this is that as a starting point for our directed evolution study the vanadium chloroperoxidase from the fungus *C. inaequalis* was taken. This terrestrial organism belongs to the group of dematiaceous hyphomyctes that normally grow on plants and are plant parasites; in the natural habitat of the fungus the enzyme will probably meet neutral to slightly acidic conditions. In addition to this pH effect, the bromide concentration of the fungal habitat is much lower than the concentration used in our screening (1 mM), reflected by the very high affinity of the wild-type vanadium chloroperoxidase for bromide ($K_m < 5\ \mu$M). For the VBPOs found in seaweeds the situation is different. These enzymes have evolved at 1 mM bromide and pH 8, and therefore it is not surprising that the activity of VBPO from *A. nodosum* is closer to the laboratory-evolved VCPO mutant (P395D/L241V/T343A), although a factor of 8 difference still remains to be explained. Examining the three mutation sites found in the VCPO mutant reveals that only the Pro-395 is found in a region that is conserved in the vanadium bromoperoxidases. From the crystal structures available for the vanadium bromoperoxidases we cannot give an answer as to why mutation of the proline of vanadium bromoperoxidase corresponding to Pro-395 in vanadium chloroperoxidase has not occurred *in vivo*. Site-directed mutagenesis of this residue in a vanadium bromoperoxidase may answer this question.

In summary we show the first example of directed evolution of a vanadium enzyme, increasing its turnover number maximally 100-fold at mildly alkaline pH. The changed halogenating activity may be explained by (i) a change in the electron density on the oxygens of the vanadate cofactor, in particular vanadate oxygen-2 of the peroxo-intermediate and (ii) an alteration of the electrostatics in the vicinity of the halide-binding residue Phe-397 and a change of its position. Our control mutants suggest that these effects are synergistic, a typical outcome of a directed evolution study. To further understand the higher brominating and chlorinating activities of the P395D/L241V/T343A mutant, high-resolution crystallographic studies on this mutant and especially its peroxo-intermediate are desirable. Based on the successful application of directed evolution of VCPO presented here, we also intend to generate novel VCPO activities such as enantiomeric sulfoxidation and epoxidation.

Acknowledgments—We thank Prof. Dr. H. E. Schoemaker (DSM Research, The Netherlands) and Drs. K. Willet and D. N. Williams (International Paint Ltd., United Kingdom) for stimulating discussions.

REFERENCES

1. Littlechild, J. (1999) *Curr. Opin. Chem. Biol.* **3,** 28–34
2. Dembitsky, V. M. (2003) *Tetrahedron* **59,** 4701–4720
3. Wever, R., Dekker, H. L., Van Schijndel, J. W. P. M., and Vollenbroek, E. G. M. (October 12, 1995) Patent WO 95/27009
4. Johansen, C. (February 25, 1999) Patent WO 99/08531
5. Svendsen, A. and Jorgensen, L. (April 16, 2002) U. S. Patent 6,372,465
6. Hansen, E. H., Albertsen, L., Schäfer, T., Johansen, C., Frisvad, J. C., Molin, S., and Gram, L. (2003) *Appl. Environ. Microbiol.* **69,** 4611–4617
7. Hansen, E. H., Schäfer, T., Molin, S., and Gram, L. (2005) *J. Appl. Microbiol.* **98,** 581–588
8. Ortiz-Bermúdez, P., Srebotnik, E., and Hammel, K. E. (2003) *Appl. Environ. Microbiol.* **69,** 5015–5018
9. Renirie, R., Pierlot, C., Aubry, J. M., Hartog, A. F., Schoemaker, H. E., Alsters, P. L., and Wever, R. (2003) *Adv. Synth. Cat.* **345,** 849–858
10. De Boer, E., Plat, H., Tromp, M. G. M., Franssen, M. C. R., Van der Plas, H. C., Meijer, E. M., Schoemaker, H. E., and Wever, R (1987) *Biotechnol. Bioeng. Symp.* **30,** 607–610
11. Wever, R., Tromp, M. G. M., Krenn, B. E., Marjani, A., and Van Tol, M. (1991) *Environ. Sci. Technol.* **25,** 446–449
12. Borchardt, S. A., Allain, E. J., Michels, J. J., Stearns, G. W., Kelly, R. F., and McCoy, W. F. (2001) *Appl. Environ. Microbiol.* **67,** 3174–3179
13. Messerschmidt, A., Prade, L., and Wever, R. (1997) *Biol. Chem.* **378,** 309–315
14. Renirie, R., Hemrika, W., and Wever, R. (2000) *J. Biol. Chem.* **275,** 11650–11657
15. Zampella, G., Fantucci, P., Pecoraro, V. L., and De Gioia, L. (2005) *J. Am. Chem. Soc.* **127,** 953–960
16. Wever, R., and Hemrika, W. (2001) in *Handbook of Metalloproteins* (Huber, R., Poulos, T., and Wieghardt, K., eds), pp. 1417–1428, John Wiley & Sons, Ltd., Chichester
17. Littlechild, J., Garcia-Rodriguez, E., Dalby, A., and Isupov, M. (2002) *J. Mol. Recognit.* **15,** 291–296
18. Littlechild, J., and Garcia-Rodriguez, E. (2003) *Coord. Chem. Rev.* **237,** 65–76
19. Messerschmidt, A., and Wever, R. (1996) *Proc. Natl. Acad. Sci. U. S. A.* **93,** 392–396
20. Tanaka, N., and Wever, R. (2004) *J. Inorg. Biochem.* **98,** 625–631
21. Oshiro, T., Littlechild, J., Garcia-Rodriguez, E., Isupov, M. N., Iida, Y., Kobayashi, T., and Izumi, Y. (2004) *Protein Sci.* **13,** 1566–1571
22. Hemrika, W., Renirie, R., Macedo-Ribeiro, S., Messerschmidt, A., and Wever, R. (1999) *J. Biol. Chem.* **274,** 23820–23827
23. Carter, J. N., Beatty, K. E., Simpson, M. T., and Butler, A. (2002) *J. Inorg. Biochem.* **91,** 59–69
24. Shimonishi, M., Kuwamoto, S., Inoue, H., Wever, R., Oshiro, T., Izumi, Y., and Tanabe, T. (1998) *FEBS Lett.* **428,** 105–110
25. Chen, K., and Arnold, F. H. (1993) *Proc. Natl. Acad. Sci. U. S. A.* **90,** 5618–5622
26. Leung, D. W., Chen, E., and Goeddel, D. V. (1989) *Technique* (*Phila.*) **1,** 11–15
27. Riley, J. P., and Chester, R. (1971) in *Introduction to Marine Chemistry*, pp. 60, Academic Press, London and New York
28. Claiborne, A., and Fridovich, I. (1979) *J. Biol. Chem.* **254,** 4245–4252
29. Seaver, L. C., and Imlay, J. A. (2001) *J. Bacteriol.* **183,** 7173–7181
30. Soedjak, H. S., Walker, J., and Butler, A. (1995) *Biochemistry* **34,** 12689–12693
31. Van Schijndel, J. W. P. M., Barnett, P., Roelse, J., Vollenbroek, E. G. M., and Wever, R. (1994) *Eur. J. Biochem.* **225,** 151–157
32. De Boer, E., Van Kooyk, Y., Tromp, M. G. M., Plat, H., and Wever, R. (1986) *Biochim. Biophys. Acta* **872,** 104–115
33. DeLano, W. L. (2002) *The PyMOL Molecular Graphics System*, San Carlos, CA, U. S. A
34. Macedo-Ribeiro, S., Hemrika, W., Renirie, R., Wever, R., and Messerschmidt, A. (1999) *J. Biol. Inorg. Chem.* **4,** 209–219
35. Verschueren, K. H. G., Seljée, F., Rozeboom, H. J., Kalk, K. H., and Dijkstra, B. W. (1993) *Nature* **363,** 693–698
36. De Boer, E., and Wever, R. (1988) *J. Biol. Chem.* **263,** 12326–12332
37. Chasteen, N. D. (1983) in *Structure and Bonding*, pp. 105–138, Springer Verlag, Berlin Heidelberg
38. Tanaka, N., Hasan, Z., and Wever, R. (2003) *Inorg. Chim. Acta* **356,** 288–296
39. Heck, R. F., and Nolley, J. P., Jr. (1972) *J. Org. Chem.* **37,** 2320–2322
40. Cabri, W., and Candiani, I. (1995) *Acc. Chem. Res* **28,** 2–7